

Analysis of Output Voltage in Contact Separation Triboelectric Nanogenerator: A Numerical Calculation-Based Study for Ships

Ede Mehta Wardhana¹, A.A. Masroeri², Brivo Rafanki³

(Received: 16 July 2024 / Revised: 10 August 2024 / Accepted: 19 August 2024)

Abstract— Triboelectric Nanogenerator (TENG) is an innovative technology that harnesses the triboelectrification phenomenon to generate electricity through the Contact Separation mode, where two materials with triboelectric properties interact. TENG can generate electricity at low frequencies. In the context of ship engine vibrations, the application of TENG with the Contact Separation mode can convert mechanical vibration energy from vibrations generated in the ship engine room into additional electrical power sources. The principle of TENG operation focuses on changes in triboelectric charge during the contact, separation, and compression processes. This study uses parameters commonly encountered in ships, namely low-frequency vibrations, as well as limitations imposed by classifications and regulations on these vibrations. Parameters used to analyze suitable modes for application in ships vary, namely frequencies ranging from 1 to 30 Hz and displacement distances ranging from 0.5 to 2 mm with intervals of 0.5 mm, resulting in voltages ranging from 0.01 to 1.55 V. After obtaining suitable modes, this study will match the modes for application on ships with a frequency of 50 Hz and displacement distances varied from 7 to 25 mm using FEP and Silicone materials, resulting in voltages ranging from 13.20 to 249.20 V. The results of this research can provide guidance for the development of TENG technology on ship engines to enhance energy efficiency and sustainability in the maritime sector.

Keywords— contact-separation, FEP, frequency, triboelectric nanogenerator

I. INTRODUCTION

The consumption of natural resources, such as petroleum, contributes to environmental pollution, making carbon emission reduction crucial to achieving carbon neutrality and finding non-emissive renewable energy sources. Various renewable energies, such as solar energy, wind energy, and blue energy (water), are being extensively explored and researched. Additionally, due to the vastness of the oceans, the development and implementation of ocean energy have become important approaches to addressing the increasingly serious energy issues^[1].

The Triboelectric Nanogenerator (TENG), discovered by Z.L. Wang in 2012, is based on the relationship between the contact electrification effect and electrostatic induction. Two different materials can generate

triboelectric effects with the presence of forces affecting the distance between the materials. However, in the industrial context, this can have negative consequences as the electrostatic charge induced by the penetration of the two materials can lead to sparks, dielectric damage, electronic damage, and even explosions. From an energy harvesting perspective, two triboelectric materials separated will produce electrostatic charges as capacitive energy devices. This leads to friction machine generators and Van de Graaff generators, thus, these devices can be referred to as Triboelectric Nanogenerators (TENG). In the maritime field, Triboelectric Nanogenerators (TENG) can be used for energy harvesting, as discussed in the paper by Changsui Song et al. "Recent advances in harvesting marine energy with Triboelectric Nanogenerators", and can also be utilized as monitoring and sensing devices by utilizing electrostatic induction as signals^[2].

TABLE 1.
A COMPARISON OF TENG WITH OTHER ENERGY HARVESTERS HAS BEEN DISCUSSED BY HAO ET AL. (2022).

	Efficiency	Charge Density	Cost	Low Freq.	Environment Adoption
Solar Panel	18-38%	47-66 W m ⁻²			
EMG	30-66%	10-20 W m ⁻²			Fit
TENG	50-98%	100-500 W m ⁻²	Fit	Fit	Fit

Ede Mehta Wardhana Departement of Marine Technology, Sepuluh Nopember Institute of Technology, Surabaya, 60111, Indonesia.
Agoes Ahmad Masroeri Department of Marine Technology, Sepuluh Nopember Institute of Technology, Surabaya, 60111, Indonesia

Brivo Rafanki Departement of Marine Technology, Sepuluh Nopember Institute of Technology, Surabaya, 60111, Indonesia. E-mail: brivofanki@gmail.com

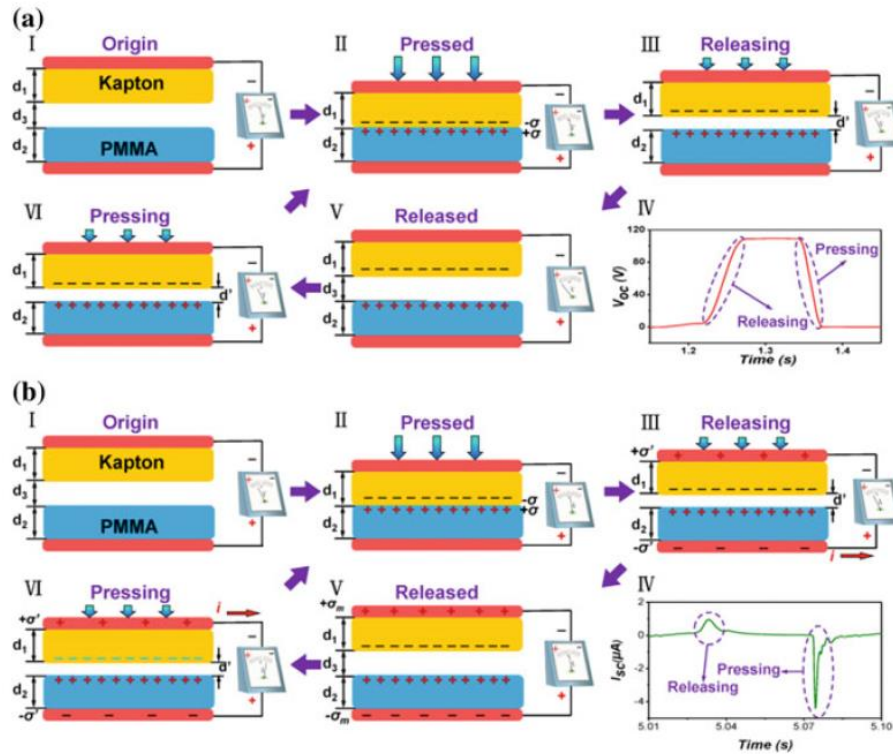


Figure 1. Principle of CS-TENG operation. a. Open-circuit condition. b. Short-circuit condition.

Ship engine vibrations constitute external forces for TENG, thus the principle of the device with two materials, i.e., vertical movement, will generate electrical output. The electrical output of this device depends on the materials used, determining different pull forces on electrons from the materials. When two materials are brought close together, electric charges will be induced on the device's surface, producing a potential difference, then electrons are transferred to the material with a more electronegative element, such as copper in the cable.

Compared to solar energy, TENG offers the advantages of continuous operation, low cost, and strong environmental adaptability. TENG can also be utilized for low-frequency wave energy compared to Electromagnetic Generators (EMG), which are essentially more suitable for harvesting high-entropy energy. The characteristics of TENG have other advantages in harvesting marine energy, as outlined in **Table 1**^[3].

Research on TENG technology is expected to become an alternative power generator and be applied in the long term at an economical price. The submitted paper presents the results of energy harvesting from TENG by selecting specific materials capable of generating electricity and the benefits of the electricity produced for application in ship components/systems. This can be further developed into renewable energy for everyday life.

II. BASIC THEORY

A. Contact Separation Triboelectric Nanogenerator Mode.

The working principle of TENG with the CS mode can be defined by combining electrical contact and electrostatic induction^[4]. **Figures 1a** and **1b** illustrate the outputs of open-circuit voltage (VOC) and short-circuit current (ISC), respectively.

Initially, in the starting position, there is no charge or induction generated by TENG, resulting in no potential difference between the two materials (**Figure 1a-I**). With the application of an external force, the two polymers will come into contact with each other, leading to the transfer of charges on the material surfaces due to the triboelectric effect. Following the triboelectric series, which is a list of materials based on their tendency to gain or lose charge, electrons are transferred from polymethyl methacrylate (PMMA) to Kapton, resulting in a negative charge on the Kapton surface and a positive charge on the PMMA surface. The insulating properties of the polymer allow the retention of triboelectric charges for a long time, for hours or even days, on the surface. At this stage, however, there is no electrical potential difference between the two electrodes (**Figure 1a-II**).

Once the two polymers are separated, a potential difference will form between the two electrodes under open-circuit conditions because the opposing triboelectric charges are separated (**Figure 1a-III**). The VOC value will continue to increase until its maximum point as Kapton returns to its original position (**Figure 1a-IV, V**). If the two electrodes are shorted, any potential difference formed due to the separation of the two polymers will cause electrons to move from the top electrode to the bottom electrode, resulting in instant positive current during the releasing process (**Figure 1b-III**). As a result, electrons will be pushed from the bottom electrode back to the top electrode, reducing the induced charge amount (**Figure 1b-VI**). This process corresponds to the instant negative current (**Figure 1b-V**). When the two polymers come into contact again, all induced charges will be neutralized (**Figure 1b-II**)^[5].

B. Capacitive Equation and V-Q-x Relationship in CS-TENG

Every triboelectric energy harvester consists of a pair of opposing materials (referred to as tribo-pairs). The

$$E_{air} = \frac{-\frac{Q}{S} + \sigma(t)}{\epsilon_0} \quad (7)$$

distance (x) between these two triboelectric layers can vary depending on the mechanical force. When the two materials come into contact with each other, it results in contact electrification where the contact surfaces of the two triboelectric layers will have opposite static charges (tribo-charges). In addition to the pair of material layers, there are two electrodes as isolators that ensure charges are only transferred through the circuit. By definition, if the charge transferred from one electrode to the other is Q, one electrode will have a charge transferred of -Q, and the other electrode will have a charge transferred of +Q, as discussed in the initial paragraph^[6].

The theoretical calculation related to the real-time power generated from TENG is the relationship between three important parameters called the V-Q-x relationship, including: the voltage (V) between the two electrodes, the amount of charge transferred (Q) between the two electrodes, and the separation distance (x) between the two triboelectric surfaces. Calculations using the V-Q-x relationship model of CS-TENG can be performed by deriving formulas based on the theory of electrostatics capacitance^[7]. From the Capacitance equation (C), it can be converted into a matrix equation to include the constant permittivity value (ϵ_0), the surface area of the TENG (S), and the distance between the two materials (d):

$$C = Q/V \quad (1)$$

$$Q = C \times V = \frac{\epsilon_0 S}{d} V \quad (2)$$

$$\frac{Q}{S} = \sigma = D = \frac{\epsilon_0 V}{d} \quad (3)$$

Where σ represents charge density, it can also be interpreted as electric flux density (D). From the equation above, it can also be transformed into the equation of electric field (E):

$$E = \frac{\sigma}{\epsilon_0} \quad (4)$$

$$E = \frac{V}{d} \quad (5)$$

Because the surface area (S) of the metal is several times larger than the separation distance between the two electrodes ($d_1 + d_2 + x$), it is assumed that the electrodes are infinitely sized. Based on this assumption, the charge on the electrodes will be uniformly distributed over the entire inner surface of both metals. Inside the dielectric material and air gap, there is an electric field perpendicular to the electrode surface, where the transferred charge value is positive on metal 2. The

electric field strength in each region is given by Gauss's theorem:

Inside dielectric 1:

$$E_1 = -\frac{Q}{S\epsilon_0\epsilon_{r1}} \quad (6)$$

Inside air dielectric:

Inside dielectric 2:

$$E_2 = -\frac{Q}{S\epsilon_0\epsilon_{r2}} \quad (8)$$

The voltage between two electrodes is obtained from the equation:

$$V = E_1 d_1 + E_2 d_2 + E_{air} x \quad (9)$$

From the equation mentioned above, we obtain the V-Q-x relationship for CS-TENG dielectric-to-dielectric as follows:

$$V = -\frac{Q}{S\epsilon_0} \left(\frac{d_1}{\epsilon_{r1}} + \frac{d_2}{\epsilon_{r2}} + x(t) \right) + \frac{\sigma x(t)}{\epsilon_0} \quad (10)$$

Meanwhile, for CS-TENG conductor-to-dielectric, the V-Q-x relationship can be written as follows:

$$V = E_2 d_2 + E_{air} x \quad (11)$$

$$V = -\frac{Q}{S\epsilon_0} \left(\frac{d_2}{\epsilon_{r2}} + x(t) \right) + \frac{\sigma x(t)}{\epsilon_0} \quad (12)$$

The equation above could be further derived if the type of TENG mode and the external forces where TENG is applied differ. In this case, TENG will be applied on a ship with the simplification of external force formulas using simple harmonic motion equations.

C. TENG Material

The nature of triboelectrification involves the transfer of electrons due to physical contact between two materials. The direction of electron movement is determined by the difference in electron affinity between the two materials. One material with the highest electron affinity (electron acceptor) will attract electrons from the other material (electron donor). With each role identified, they can be classified based on the triboelectric series (**Figure 2**)^[8].

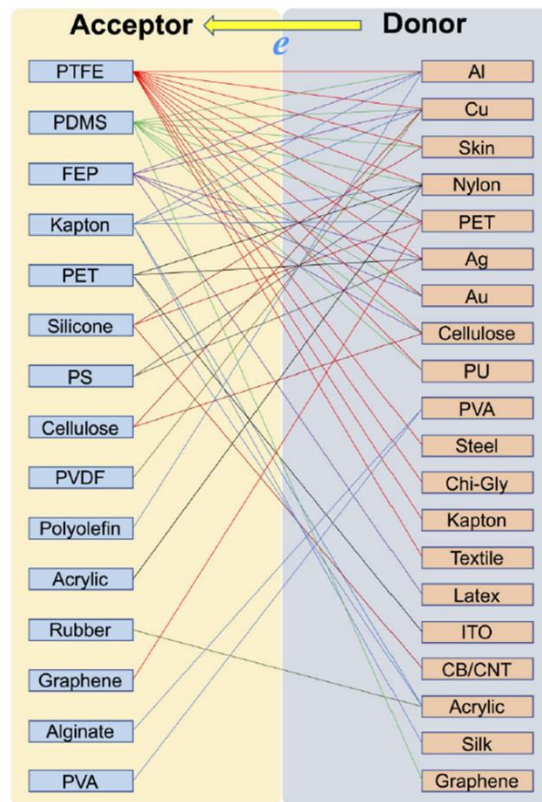


Figure 3. The relationship of triboelectrification between electron acceptors and donors is based on the triboelectric series (Zhang and Olin, 2020).

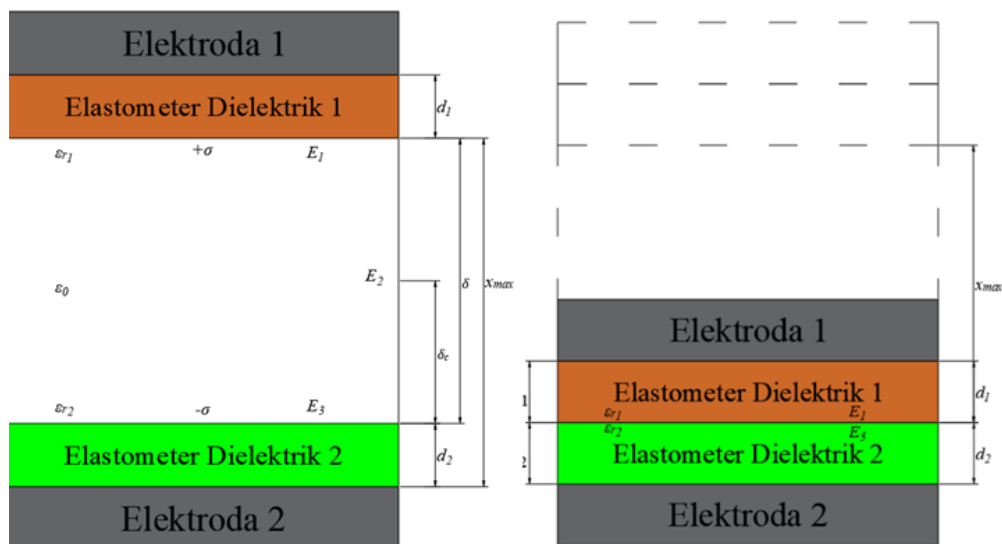


Figure 2. The caption for the image to indicate its parameters.

III. Results and Discussion

A. Material Parameter

Determining the material to be studied, where the material below or dielectric elastomer 2 must be flexible or compressible, as flexibility of the material will affect the calculated output voltage. The surface area of the material will also affect the generated voltage. The

dielectric constant values of each material must be higher to induce positive or negative electron polarization according to the conditions that will ultimately produce alternating current. The materials used in the numerical analysis of TENG are obtained from secondary data (books & journals) with parameters such as the **table 2**.

TABLE 2.
 PARAMETERS THAT WILL BE USED IN VOLTAGE CALCULATIONS.

Parameter	
Material area S	25,0 cm ²
Material thickness 1 d_1	1,0 mm
Material thickness 2 d_2	1,0 mm
Air dielectric constant ϵ_0	1,0
Material dielectric constant 1 (FEP) ϵ_{r1}	2,2
Material dielectric constant 2 (Silikon) ϵ_{r2}	7,2
Resistance R	1M Ohm
Effective thickness d_0	0,00075 mm

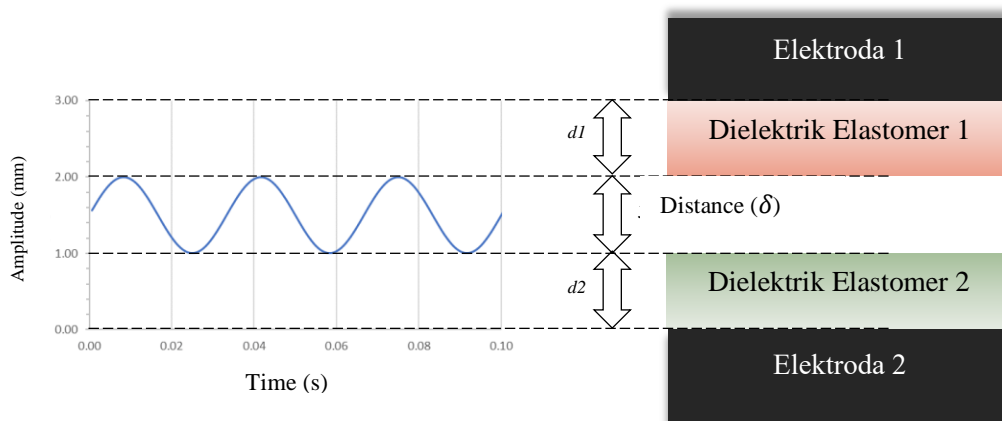


Figure 4. The graph showing positions at specific times with each displacement distance at a frequency of 15 Hz.

The parameters above are primarily for the materials. In this calculation, the effective thickness constant d_0 is defined as the sum of the thicknesses of all given materials divided by the dielectric constant of the material ϵ_{ri} , where the calculation here uses the dielectric constants of material 1, which is FEP (Fluorinated ethylene propylene), and material 2, which is silicon.

The use of silicon as dielectric elastomer 2 is chosen because of its material flexibility, enabling it to support compression mode. Therefore, it can be represented as the formula below:

$$d_0 = \sum_{i=1}^n \frac{d_i}{\epsilon_{ri}} \quad (13)$$

B. Vibration Parameter

Parameters of vibration are needed to determine the distance between materials, displacement, vibration velocity, and frequency. Vibration parameters are crucial here as they will affect the output provided by the TENG, parameters such as the **table 3**.

TABLE 3.
 THE VIBRATION PARAMETERS THAT ACT AS THE EXTERNAL FORCE FOR TENG.

Parameter	
Initial separation distance x_0	1,5 mm
Maximum displacement x_{max}	2,5 - 4 mm
Amplitude Amp	0,25 - 1 mm
Vibration frequency f	1 - 30 Hz
Number of periode	5
Vibration periode	0,033 s
Time t	0,167

C. Calculation of TENG Output

In the calculation for CS-TENG, the equation provided has been developed by Z.L. Wang (2016) and validated based on experiments in the journal by E.M. Wardhana et al. (2020) [9]. **Figure 3** shows dielectric elastomers with thicknesses d_1 and d_2 , each having relative dielectric constants ϵ_{r1} and ϵ_{r2} , laminated with opposing air layers (distance: δ and dielectric constant: ϵ_0) as the triboelectric layers.

Two electrodes are placed on the bottom and top sides of the dielectric elastomer as conduits for electrical current (typically exhibiting conductive properties). The varying separation distance between the two dielectric elastomers depends on the amplitude A and frequency f of the vibration. Charges can be induced on the surface of the triboelectric layer with charge density σ during contact-separation. The electric potential difference Φ between the two electrodes is generated when the separation distance $x(t)$ occurs due to the external force.

1) Calculation of TENG Movement

Figure 4 illustrates the movement of material 2 driven by the external force, forming a sinusoidal graph with predetermined displacement distances of 0.5, 1.0, 1.5, 2.0 mm at the frequencies provided in Table 8. The movement of the TENG material can be determined using the equation of simple harmonic motion, which can be derived as follows:

$$x(t) = Amp * \sin(\omega t + \theta) \quad (14)$$

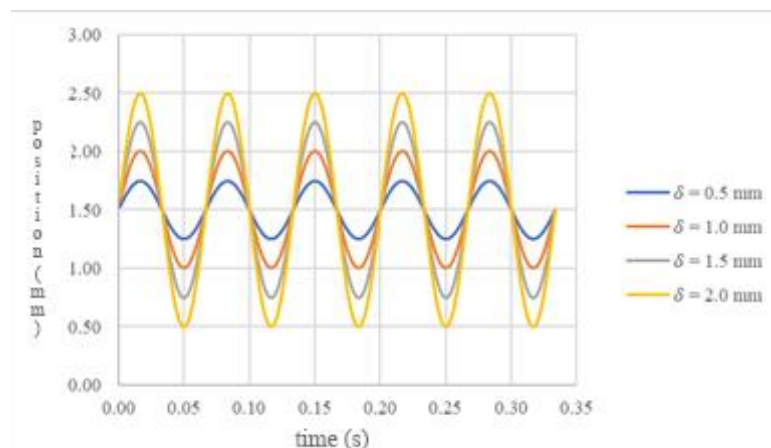


Figure 5. The graph depicts the displacement and a sketch of TENG movement with a separation distance of 1.0 mm at a frequency of 10 Hz.

Where $x(t)$ represents the position at a specific time, Amp is the amplitude, and θ is the initial position of the TENG before movement. Equation 14 enables researchers to compute using Matlab software to aid in determining the specified iterations. **Figure 5** illustrates the material's position at a given time. Due to the initial separation distance, the displacement provided will begin at 1.5 mm each, as per Equation 14. This will affect the voltage generated because both the displacement and the initial separation distance will influence the mode that occurs.

2) Theoretical Calculation of Output Voltage

The electrical potential V can conduct electrons back and forth between the two electrodes, thus the electricity generated is AC. Therefore, this relationship can be formulated as follows:

$$\Delta\phi = Ed \quad (15)$$

$$D = \epsilon E \quad (16)$$

$$D = \sigma \quad (17)$$

$$Q = \sigma A = DA \quad (18)$$

As the position of the two materials moves, it will result in a potential difference that can be expressed as follows:

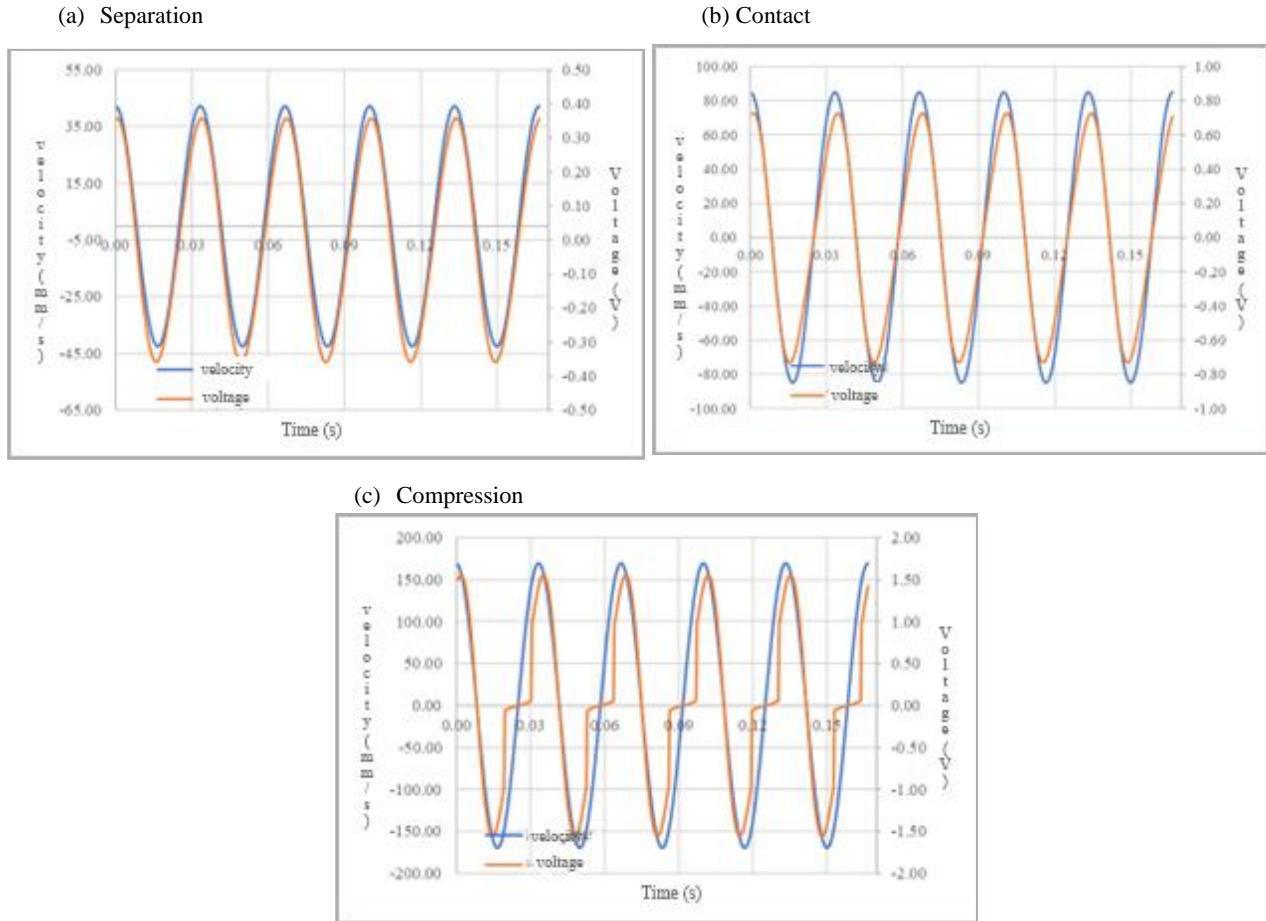


Figure 6. The results of voltage and vibration velocity calculations over time at $\delta =$ (a) 0.5 mm; (b) 1.0 mm; (c) 2.0 mm with $f = 30$ Hz.

$$C = \frac{Q}{\Delta\phi} \quad (19)$$

$$C = \frac{DA}{(x(t) + d_0) \frac{D}{\epsilon_0}} \quad (20)$$

$$C = \frac{\epsilon_0 A}{x(t) + d_0} \quad (21)$$

During the compression mode where the position $x(t) < d_1$, it means that material 1 is pressing material 2 to the position given in equation 20. Because it is compressed, the thickness of material 2 $d_2 = 0$, thus the capacitance can be expressed as follows:

$$C = \frac{\epsilon_0 A}{x(t) + \frac{d_1}{\epsilon_{r1}} + \frac{d_2}{\epsilon_{r2}}} \quad (22)$$

$$C = \frac{\epsilon_0 (\epsilon_{r1} + \epsilon_{r2}) A}{x(t) + d_2} \quad (23)$$

Then Kirchhoff's law and Ohm's law also apply in the principle of TENG, so their equations can be derived as follows:

$$V_r + V_{ma} = 0 \quad (24)$$

$$V_r = Ri \quad (25)$$

$$i = i_{ma} \quad (26)$$

$$q_{ma} = K_{ma} C_{ma} V_{ma} \quad (27)$$

Where R is the internal resistance (in this research, the internal resistance is assumed), ma refers to the capacitance element in air dielectric and dielectric elastomer, and K_{ma} is the coefficient between the air layer and the dielectric elastomer and depends on $dx(t)/dt$ before contact. The coefficient can be expressed as follows:

$$K_{ma} = K_f \frac{dx(t)}{dt} = K_f \frac{d}{dt} \{x_{max}\} = \frac{d}{dt} \{(1 - \cos 2\pi ft) Amp\} \quad (28)$$

From equation 24, it can be derived as:

$$V_r = -V_{ma} \quad (29)$$

$$Ri = -\frac{q_{ma}}{K_{ma} C_{ma}} \quad (30)$$

$$i = \frac{dq}{dt} = \frac{dq_{ma}}{dt} \quad (31)$$

$$\frac{dq_{ma}}{dt} = -\frac{1}{RK_{ma} C_{ma}} q_{ma} \quad (32)$$

With the equation above, the voltage generated by the TENG can be obtained through time intervals or integration.

D. Results of Theoretical Calculation of Output Voltage

In the theoretical calculation of the output voltage generated by CS-TENG, it is recorded according to the variations in frequency, displacement, and the occurring mode. The output voltage can provide information regarding the performance of TENG and its potential as an energy source. Below are the respective output voltages corresponding to each mode. Therefore, it can be determined whether these outputs would be suitable if applied inside the engine room of a ship, where the engine room serves as a source of vibration.

1) Voltage in Separation Mode

The separate mode can be considered when material 1 & material 2 are not in contact or $x(t) > d_2$. In this study, $\delta = 0.5$ mm. As illustrated in **Figure 7**, there is no contact between the materials, and as each material approaches and then moves away, there is empty air space between

them. In the calculation of capacitance, equation 20 can be used because the conditions always remain separate. The voltage graph shows streamline, indicating perfect electrical conduction. However, in ship engine room applications, this would be impossible without a support/spring connecting the two materials. The calculation results for $\delta = 0.5$ mm with $f = 30$ Hz (Figure 10(a)) yield a maximum voltage of $V_{max} = 0.36$ V. In this section, the effect of the separation speed of the materials on the output voltage of the TENG is examined. **Figure 6(a)** shows the time variation of the output voltage and separation speed. The phase between them is almost simultaneous, especially in the separation mode. The output voltage reaches maximum/minimum values when the separation speed is maximum/minimum.

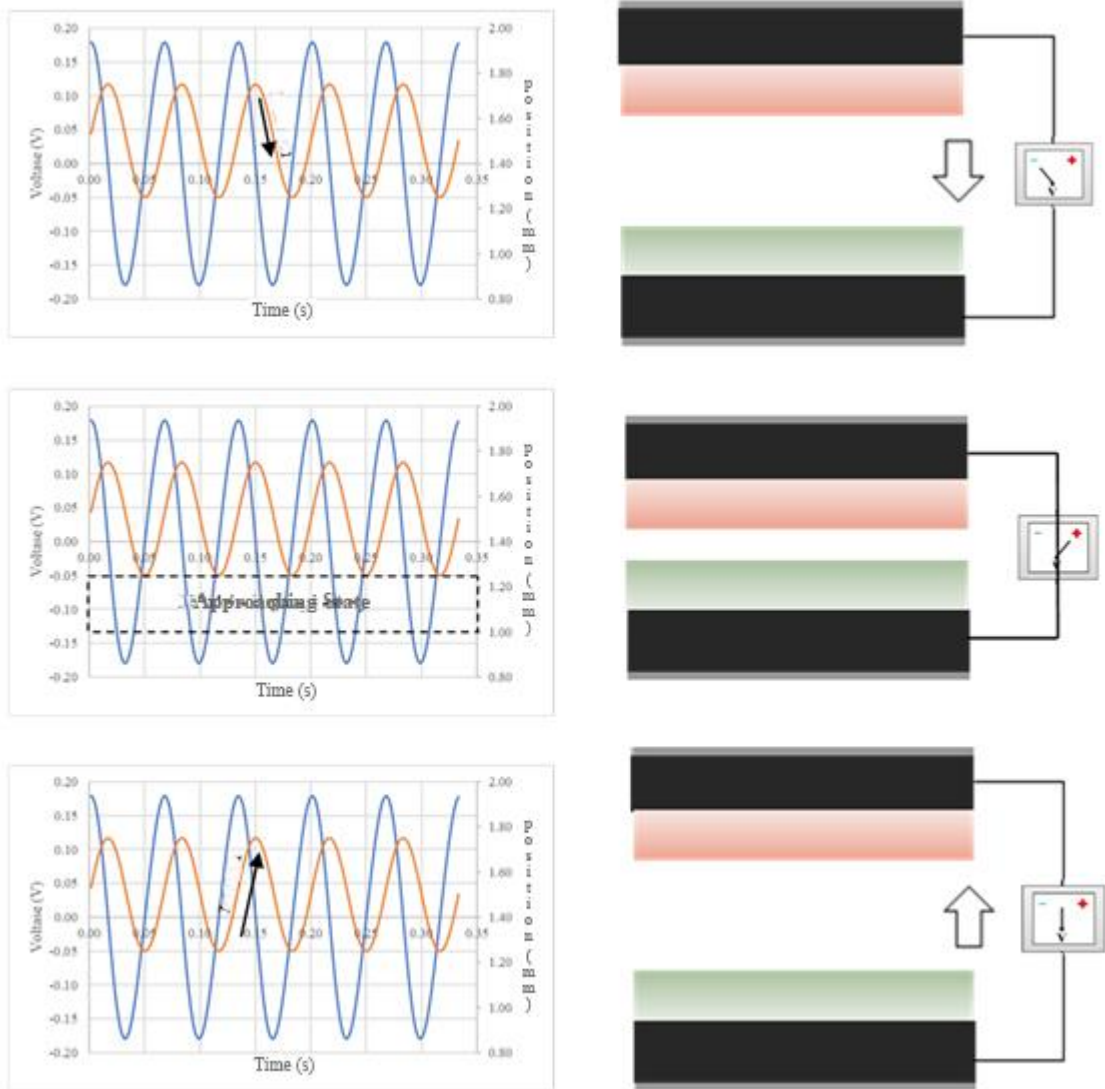


Figure 7. Graph of the relationship between voltage (V), position (x), and time (t) at $\delta = 0.5$ mm, $f = 15$ Hz.

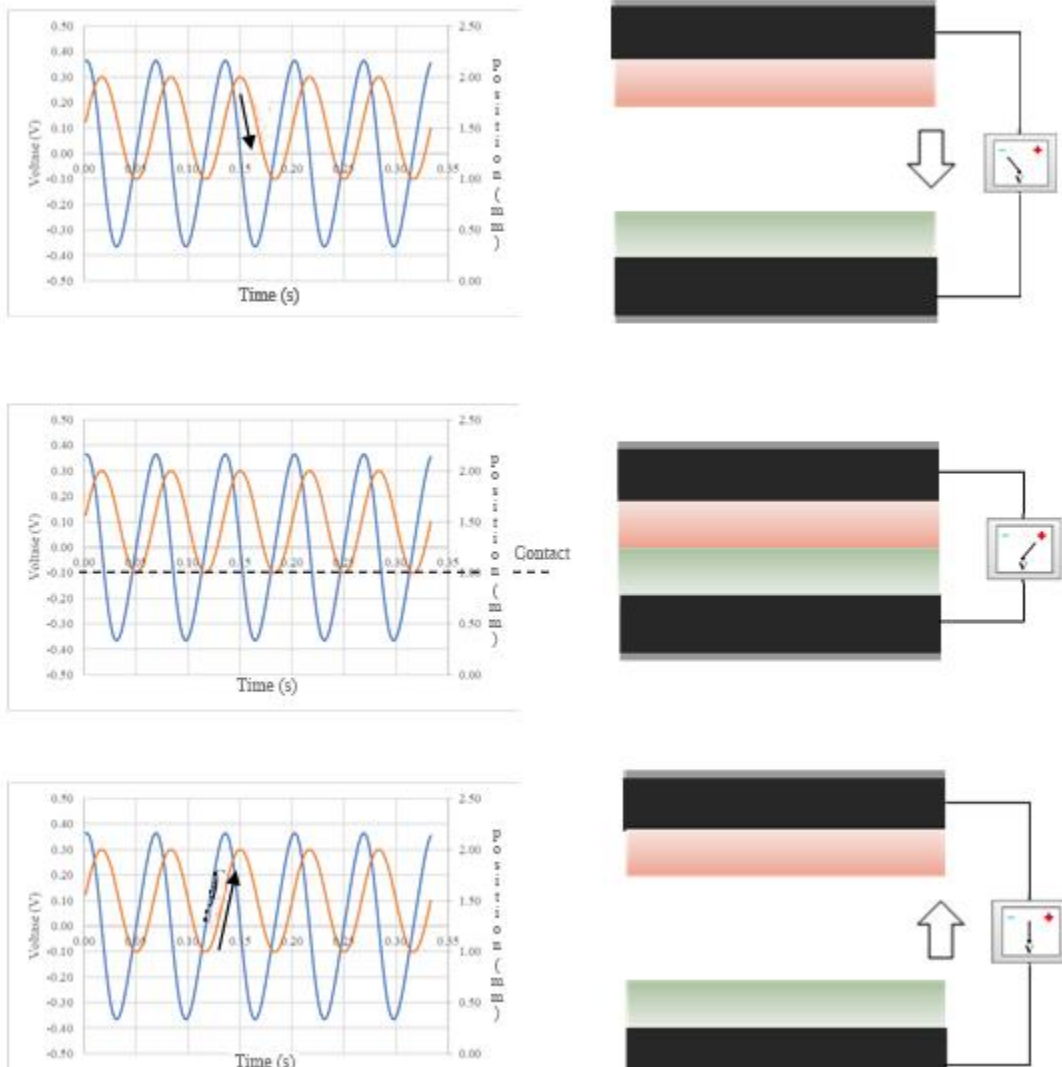


Figure 8. Graph of the relationship between voltage (V), position (x), and time (t) at $\delta = 1.0 \text{ mm}$, $f = 15 \text{ Hz}$.

2) Voltage in Contact Mode

This study will focus on the contact mode because this mode allows for application without the use of supports/springs since the starting point will follow the Earth's gravity (if the TENG position is parallel to the direction of the Earth's gravitational force). This mode can be considered as contact when each material touches each other at $x(t)=d_2$ as shown in **Figure 8**. This mode uses equation 20 to calculate its capacitance because the thickness of material 2 does not decrease. **Figure 6(b)** shows a graph with parameters $\delta = 1.0 \text{ mm}$, $f = 30 \text{ Hz}$. Compared to the separate mode, this mode has a higher output voltage, namely $V_{max}=0.73V$. The characteristic of output voltage to its velocity remains the same as the separate mode, where the maximum or minimum velocity will result in maximum or minimum output voltage values as shown in **Figure 6(b)**. This mode is still considered feasible for application on ships. Eventually, each material will follow the external force provided by the vibration source on the ship, namely the engine room, and will come into contact with each other.

3) Voltage in Compression Mode

The compressed mode calculation in this study is to determine the output voltage when the material is compressed, where $x(t)<d_2$. As shown in **Figure 9**, the graph indicates the voltage value when $x(t)<d_2$, where the

current flows towards the positive direction but the voltage value approaches zero until the material is no longer compressed, indicating a decrease in the polarity level between the materials in that condition. **Figure 6(c)** shows the maximum output voltage value $V_{max}=1.55V$ with parameters $\delta = 2.0 \text{ mm}$, $f=30\text{Hz}$. The velocity during compression appears to be constant due to the flexibility of material 2. Therefore, it can be concluded that in all modes, the greater the separation/displacement given, the greater the resulting value. However, if the displacement is too large, it will affect the weakening of the charge transfer.

4) Maximum and Average Voltage on Frequency Variation

In this section, the researcher discusses the maximum voltage (**Figure 10**) and average voltage (**Figure 11**) generated by the TENG. The calculation results show variations in voltage for each frequency and displacement. It explains that the higher the frequency, the higher the resulting voltage, as well as the displacement. This is because the constant dielectric constants of each dielectric

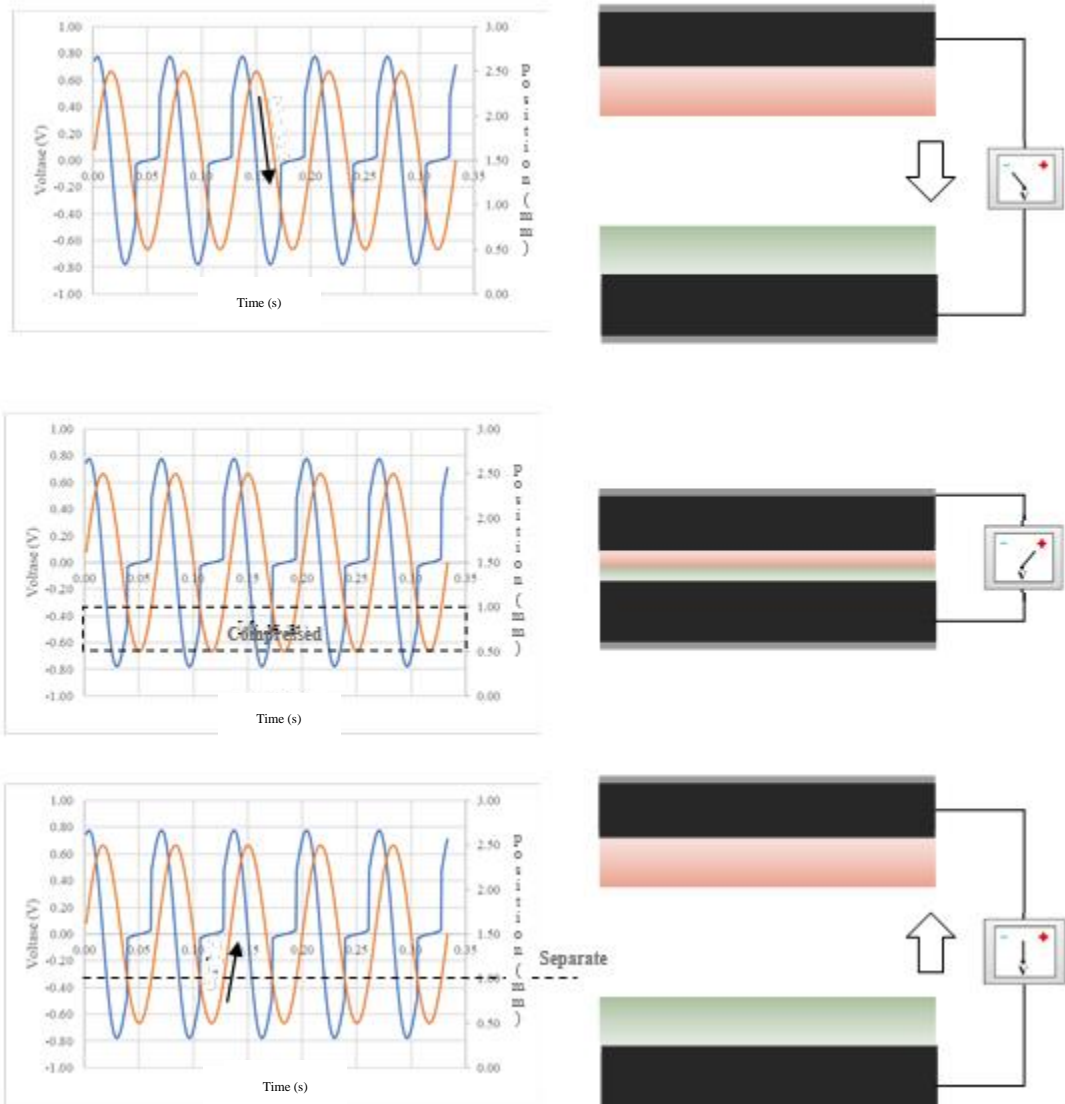


Figure 9. Graph of the relationship between voltage (V), position (x), and time (t) at $\delta = 2.0$ mm, $f = 15$ Hz.

elastomer are also related to the charge displacement that

separation distance is assumed to be constant at 0.5 mm to

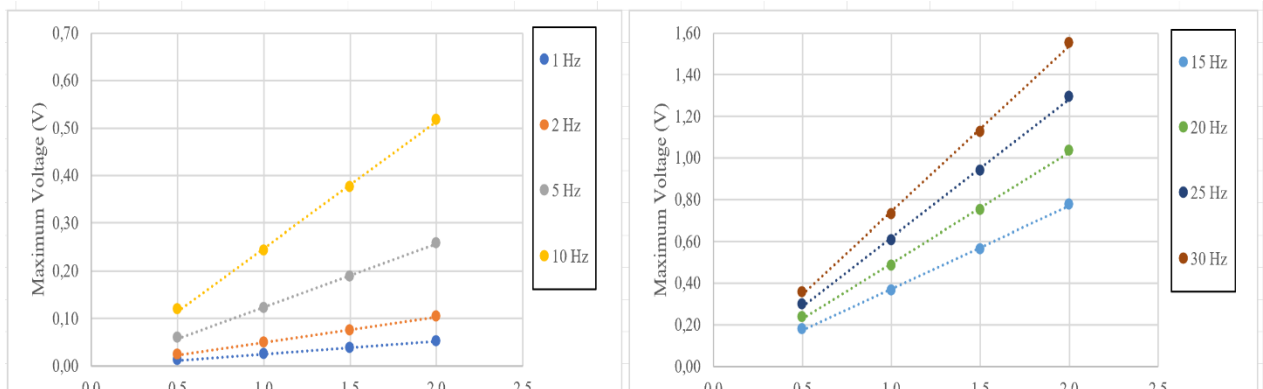


Figure 10. Maximum voltage against displacement at each frequency.

occurs when moving according to the external force.

The three modes that occur, separation, contact, and compression, are influenced by the displacement distance δ and the initial separation distance δ_c . The initial

calculate which modes would be suitable for application on a ship. The compression mode is the largest in this study because it has a larger displacement distance, providing more space for charge transfer between

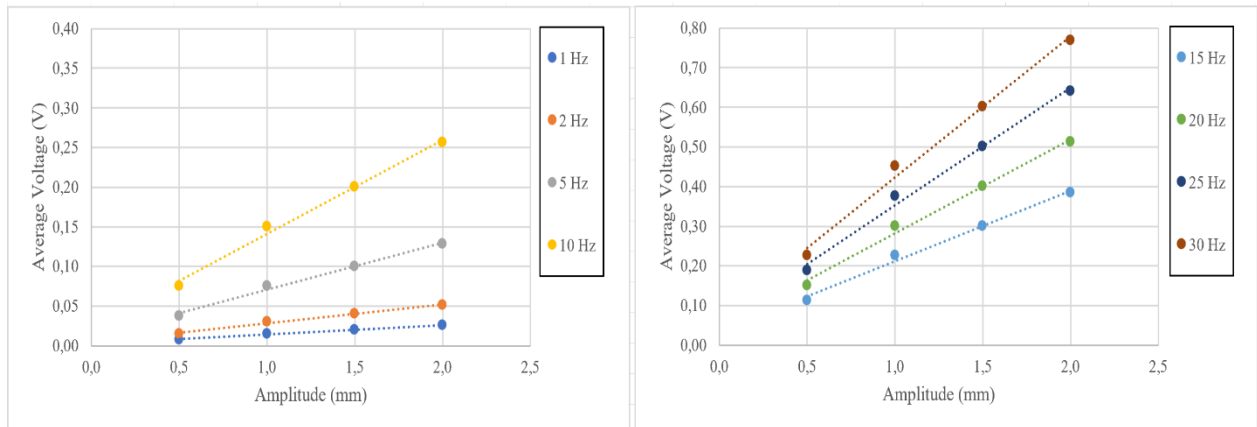


Figure 10. Average voltage against displacement at each frequency.

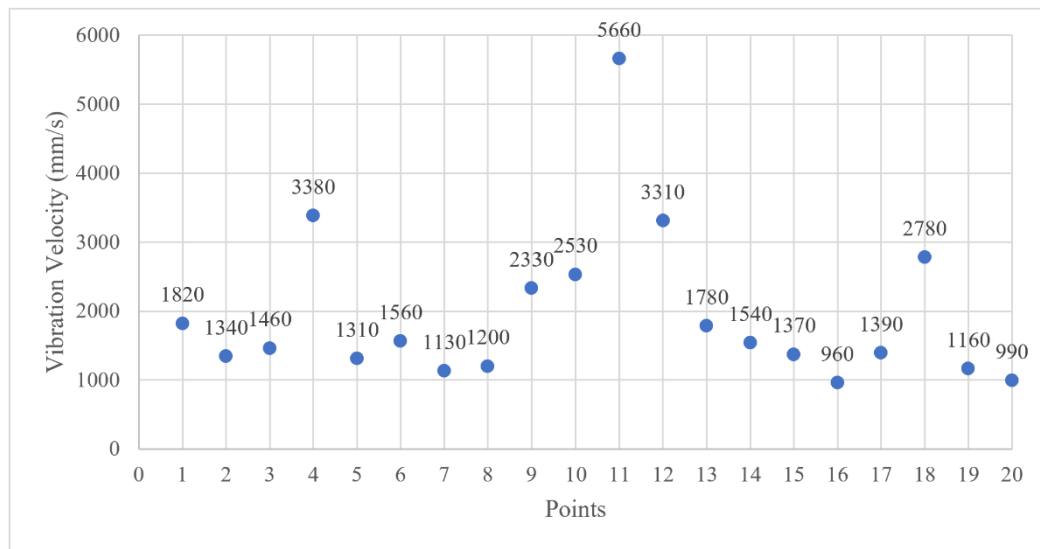


Figure 9. The measurement results of vibration velocity in the engine room of KMP Dharma Rucita.

materials. Despite compression mode being the largest, the stability of the transmitted voltage becomes one of the important parameters to consider. Therefore, the contact mode is the most suitable for application on a ship. The frequency given refers to the low-frequency produced by the engine room, as typically vibrations in the engine room experience low oscillation.

E. Application in the Engine Room of KMP Dharma Rucita

Figure 12 shows the measurement results of vibration velocity at 20 points in the engine room of KMP Dharma Rucita with frequencies recommended by the regulator or classification, ranging from 1 to 50 Hz. Points 1,2,4 and 5,8,12 are located on engine 1 and engine 2 intake, points 3,7,11 and 6,9,10 are located on the engine gearbox 1 and 2. Points 17,18 and 19, 20 are for shaft 1 and 2 on the fore, while 13,14 and 15,16 are for shaft 1 and 2 on the aft.

TENG can be effectively utilized as a renewable energy source by harnessing the vibrations in the engine room as an external force to drive its materials. In this case, the researcher will use parameters as discussed previously in Table 2 and Table 3. With a displacement distance δ ranging from 5 to 25 mm and a frequency assumed to be the standard electrical load frequency in Indonesia, which is $f = 50$ Hz. With these parameters, it is expected to be applicable with the vibration speeds provided in the above

graph, with the condition that the initial separation distance δc should be half of the displacement distance.

Figure 13 illustrates the voltage graph against displacement, where the value provided indicates that the voltage will increase as the displacement increases. Because in the equations and simulations provided earlier, there is no limit if the displacement continues to be increased. However, the stability of the output voltage will be apparent because each material/dielectric elastomer has a limit to the charge transfer at a certain position. Therefore, the dielectric constant value must be considered if you want to increase the displacement to achieve voltage stability.

The calculation for applying it in the ship's engine room uses the contact mode. Figure 14 is an example showing the position graph against time where 0 – 1 mm represents the thickness of material 1, and 11 – 12 mm represents the thickness of material 1, and the initial separation is 5.0 mm. According to its principle, the minimum value of the position is equal to material 2, which means it's in the contact mode. Figure 15 shows the vibration speed graph against displacement, where its value is directly proportional to the displacement. The larger the displacement, the greater the vibration speed generated, provided the frequency remains the same.

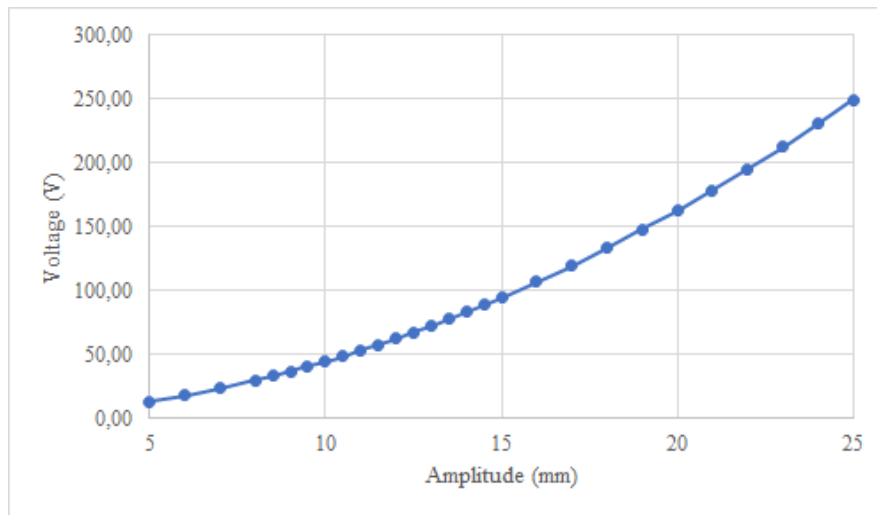


Figure 13. Voltage output graph in terms of displacement variation.

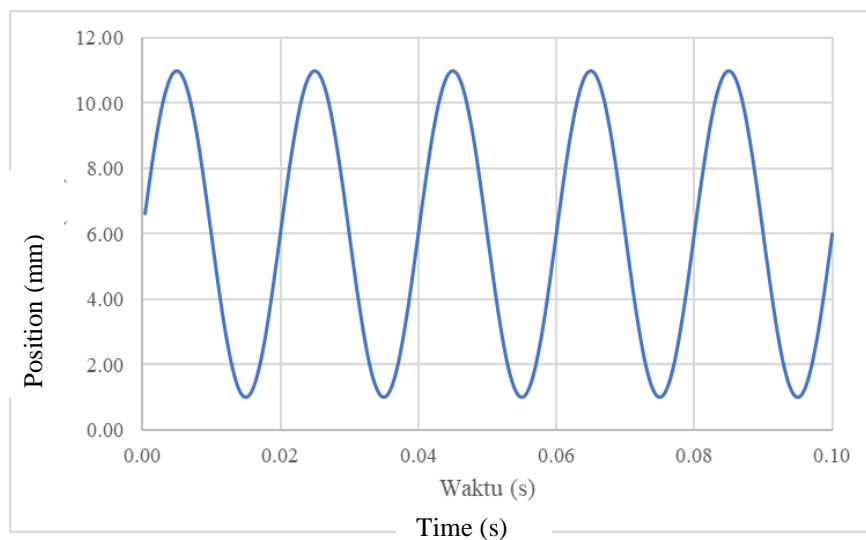


Figure 12. Position vs. time graph at $a = 10,0$ mm and $f = 50$ Hz.

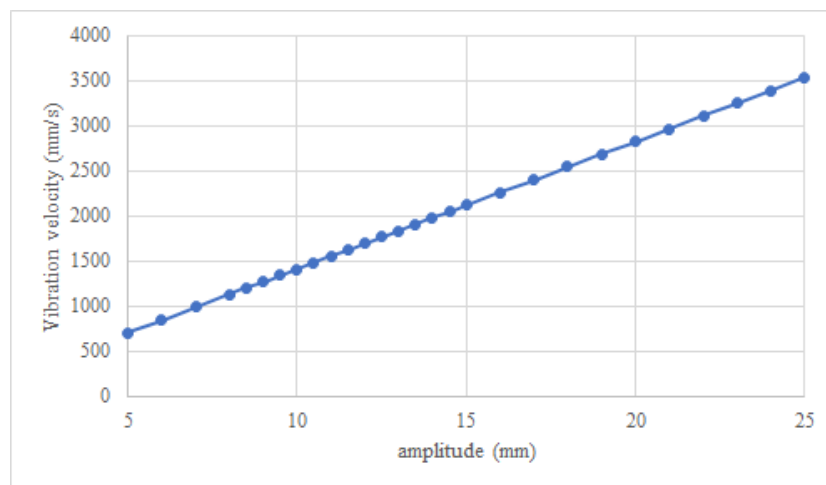


Figure 11. Graph of vibration velocity vs. time for various displacements.

IV. Conclusion

Based on our findings, the output voltage from the *Triboelectric Nanogenerator* (TENG) with frequencies varies from 1 – 30 Hz and amplitude of 0,5; 1,0; 1,5; 2,0 are used for the obtaining the TENG voltage modes of (*separation, contact and compression*). Those results are as follows : **1 Hz:** 0,01 V; 0,02 V; 0,04 V; 0,05 V | **2 Hz:**

0,02 V; 0,05 V; 0,08 V; 0,10 V | **5 Hz:** 0,06 V; 0,12 V; 0,19 V; 0,26 V | **10 Hz:** 0,12 V; 0,24 V; 0,38 V; 0,52 V | **15 Hz:** 0,18 V; 0,36 V; 0,56 V; 0,78 V | **20 Hz:** 0,24 V; 0,49 V; 0,75 V; 1,04 V | **25 Hz:** 0,30 V; 0,61 V; 0,94 V; 1,29 V | **30 Hz:** 0,36 V; 0,73 V; 1,13 V; 1,55 V. After obtaining suitable modes, this study will match the modes for application on ships with a frequency of 50 Hz and

displacement distances varied from 7 to 25 mm using FEP and Silicone materials, resulting in voltages ranging from 13.20 to 249.20 V.

REFERENCES

- [1] Z. L. Wang, "Triboelectric nanogenerators as new energy technology for self-powered systems and as active mechanical and chemical sensors," *ACS Nano*, vol. 7, no. 11, pp. 9533–9557, Nov. 26, 2013. doi: 10.1021/nm404614z.
- [2] C. Song *et al.*, "Recent advances in ocean energy harvesting based on triboelectric nanogenerators," *Sustainable Energy Technologies and Assessments*, vol. 53. Elsevier Ltd, Oct. 01, 2022. doi: 10.1016/j.seta.2022.102767.
- [3] Y. Hao, X. Li, B. Chen, and Z. Zhu, "Marine monitoring based on triboelectric nanogenerator: Ocean energy harvesting and sensing," *Front Mar Sci*, vol. 9, Nov. 2022, doi: 10.3389/fmars.2022.1038035.
- [4] H. Zhang *et al.*, "A general optimization approach for contact-separation triboelectric nanogenerator," *Nano Energy*, vol. 56, pp. 700–707, Feb. 2019, doi: 10.1016/j.nanoen.2018.11.062.
- [5] X. Chen, C. Han, Z. Wen, and Y. Liu, "Theoretical boundary and optimization methodology of contact-separation triboelectric nanogenerator," *Appl Mater Today*, vol. 29, Dec. 2022, doi: 10.1016/j.apmt.2022.101685.
- [6] S. Radhakrishnan, S. Joseph, E. J. Jelmy, K. J. Saji, T. Sanathanakrishnan, and H. John, "Triboelectric nanogenerators for marine energy harvesting and sensing applications," *Results in Engineering*, vol. 15, Sep. 2022, doi: 10.1016/j.rineng.2022.100487.
- [7] H. Zhang, L. Wang, C. Zhang, J. Shu, K. Huang, and Y. Song, "A general modification of the V-Q-x relationship of the contact-separation mode triboelectric nanogenerator," *Nano Energy*, vol. 115, Oct. 2023, doi: 10.1016/j.nanoen.2023.108716.
- [8] R. Zhang and H. Olin, "Material choices for triboelectric nanogenerators: A critical review," *EcoMat*, vol. 2, no. 4. John Wiley and Sons Inc, Dec. 01, 2020. doi: 10.1002/eom2.12062.
- [9] E. M. Wardhana *et al.*, "Harvesting contact-separation-compression vibrations using a flexible and compressible triboelectric generator," *Sustainable Energy Technologies and Assessments*, vol. 42, Dec. 2020, doi: 10.1016/j.seta.2020.100869.